REDOX REPORT
2024, VOL. 29, NO. 1, 2432830
https://doi.org/10.1080/13510002.2024.2432830

Taylor & Francis
Taylor & Francis Group

Characterization of naphthoquinones as inhibitors of glutathione reductase and inducers of intracellular oxidative stress

Xiaowan Chen[a*], Yan Ma[b*], Ziming Yang[a], Dingjie Shen[a], Xia Li[a,c,d], Maowei Ni[c], Xiaoling Xu[e†] and Wei Chen [a,c,d,f†]

[a]Postgraduate Training base Alliance of Wenzhou Medical University, Zhejiang Cancer Hospital, Hangzhou, People's Republic of China; [b]Department of Scientific Research, Zhejiang Cancer Hospital, Hangzhou, People's Republic of China; [c]Zhejiang Cancer Research Institute, Zhejiang Cancer Hospital, Hangzhou, People's Republic of China; [d]Zhejiang Provincial Key Laboratory of Integrated Traditional Chinese and Western Medicine on Cancer, Zhejiang Cancer Hospital, Hangzhou, People's Republic of China; [e]Department of Radiation Oncology, Shanghai Pulmonary Hospital, Tongji University School of Medicine, Shanghai, People's Republic of China; [f]Key Laboratory of Prevention, Diagnosis and Therapy of Upper Gastrointestinal Cancer of Zhejiang Province, Hangzhou, People's Republic of China

ABSTRACT

Glutathione reductase (GR), one of the most important antioxidant enzymes in maintaining intracellular redox homeostasis, has become a novel target to suppress cancer cell growth and metastasis. In this work, we evaluated a series of naphthoquinones (NQs) as potential GR inhibitors and elucidated the mechanism of inhibition. NQ-6, one of the most potent compounds among this series, inhibited GR *in vitro* and *in vivo* and was identified as a competitive and irreversible inhibitor. The *Ki* and k_{inact} values of NQ-6 were determined to be 17.30 ± 3.63 μM and 0.0136 ± 0.0005 min^{-1}, respectively. The tandem mass spectrometric analysis revealed that the two substrate binding sites Cys61 and Cys66 of yeast GR were modified simultaneously through arylation or only Cys66 was covalently modified by NQ-6. Intracellular reactive oxygen species, collapsing of mitochondrial membrane potential and protein *S*-glutathionylation elevation were induced by NQ-6. NQs can be valuable compounds in GR inhibition and oxidative stress-related research.

KEYWORD

Glutathione reductase (GR); naphthoquinone; inhibitor; oxidative stress; *S*-glutathionylation

1. Introduction

Naphthoquinones (NQs) have been known due to their use in traditional medicine as wound-healing agents since ancient times [1]. NQs, natural compounds with a naphthalene ring, are commonly found in many animals, plants, and microorganisms [2]. Some naturally occurring NQs including plumbagin, shikonin, lapachol, juglone, and β-lapachone have exerted various activities, such as anticancer, antioxidant, anti-inflammatory, antibacterial, and antiviral [3–5].

Oxygen-free radicals, mainly, including reactive oxygen species (ROS), reactive nitrogen species (RNS) and reactive sulfur species, play a dual role in biological systems as both deleterious and beneficial species [6, 7]. Under normal physiological conditions, ROS work as many signaling molecules in the progress of cellar life activities [8], however, once the normal level is exceeded, the high level of ROS can cause damage to DNA, proteins, amino acids and lipids even shorten telomeres *in vivo* [8, 9]. ROS plays a crucial role in many diseases including cancer [7, 10]. Compared to normal cells, many malignant tumor cells have higher ROS levels, thus ROS-modulated therapeutic strategies including ROS-scavenging and ROS-boosting approaches are pursued for cancer treatment [11].

Cells have many antioxidant systems, including enzymatic and non-enzymatic. Glutathione reductase (GR) is a crucial antioxidant enzyme which generates reduced glutathione (GSH) from oxidized glutathione (GSSG) [12] and regulates the level of ROS in the cells [13]. GSH is a tripeptide molecule which consists of glutamate, cysteine and glycine, and as the most crucial small molecule antioxidant present in the cells. GSH also plays a major role in drug resistance mechanisms [14, 15]. Studies have shown that GR expression levels are higher in recalcitrant tissues [13, 16]. Therefore, GR has become a potential therapeutic target in many diseases including cancer. GR inhibitors are developed and widely used in cancer and other diseases treatment, but the effectiveness advantage is not obvious [16]. It has been reported that the induced thiol oxidative stress by GR inhibition has shown capability to cancer cell metastasis suppression and drug resistance reversal [17, 18]. Thus, it is urgent to develop and identify new GR inhibitors.

The pharmacological effect of NQs lies in their ability to react with intracellular thiol groups, affecting the activity of intracellular enzymes such as glutathione S-Transferase [19]. This study aims to evaluate NQs as a novel class of GR inhibitor with unique mechanism of action, and to test the ability of NQs induction of oxidative stress *in vitro* and *in vivo*. We have assessed the inhibitory effect of a series of commercially available NQs on GR activity and their abilities elevation of oxidative stress, explored the inhibitory effects of NQs on GR activity *in vitro* and *in vivo*, and explored the kinetic characteristics of GR inhibition by a representative NQ of this series.

CONTACT Wei Chen chenwei@zjcc.org.cn Zhejiang Cancer Hospital, 1 East Banshan Rd., Hangzhou 310022, China; Xiaoling Xu xuxiaoling@tongji.edu.cn Department of Radiation Oncology, Shanghai Pulmonary Hospital, Tongji University School of Medicine, 507 Zhengmin Rd., Shanghai, China
*These authors contributed equally to this work.
†These authors contributed equally to this work as co-corresponding authors.

2. Methods and materials

2.1. Materials

Fetal bovine serum (FBS), penicillin/streptomycin and trypsin were purchased from Gibco (Grand Island, NY, USA). DMEM growth medium, and phosphate buffered saline (PBS) were purchased from Cellmax (Beijing, China). All reagents for GR enzyme assays including yeast GR, bovine serum albumin (BSA), ethylenediaminetetraacetic acid (EDTA) tetrasodium salt hydrate, oxidized form glutathione (GSSG) and reduced form of nicotinamide adenine dinucleotide phosphate (NADPH) were purchased from Sigma-Aldrich Chemical Co (St. Louis, MO, USA). CellRox Green Reagent was from ThermoFisher Scientific. HPLC grade acetonitrile and trifluoroacetic acid (TFA) were purchased from Tedia Company, Inc. (Fairfield, OH, USA). The mass spectrometry grade trypsin was purchased from Promega Corporation (Madison, WI, USA). Anti-glutathione antibody was from Abcam (MA, USA). Naphthoquinones (NQs) were obtained from Aladdin (Shanghai, China) and MERYER Co., LTD (Shanghai, China) and prepared as 100 mM stock solutions in dimethyl sulfoxide (DMSO). Other reagents were obtained in their highest purity grade available commercially.

2.2. Cell lines and culture conditions

Human melanoma A375 cells and gastric cancer NUGC3 cells were cultured at 37°C in a humidified atmosphere of 5% CO_2 in DMEM medium supplemented with 10% FBS, 100 U/mL penicillin and 100 µg/mL streptomycin.

2.3. GR activity assay

The GR activity assays were performed as described earlier [20] using a Multiskan Spectrum microplate reader (Thermo Scientific, Waltham, MA, USA). The final volume of GR assay mixture was 150 µL and the initial GR activity was 0.2 U/mL for each sample. The standard assay mixture containing 1 mg/mL bovine serum albumin and 0.2 mM NADPH was prepared in PE buffer (100 mM potassium phosphate, 2 mM EDTA, pH 7.0). The reaction was initiated by addition of GSSG solution (final concentration 0.5 mM) and the GR activity was determined by the initial rates of NADPH consumption detected at 340 nm in 96-well plates by a microplate reader.

2.4. Screening of GR inhibitory effect by NQs

Purified yeast GR prepared in PE buffer containing 1 mg/mL BSA and 0.2 mM NADPH was incubated with various concentrations (0-32 µM) of all the purchased 17 NQs at 37°C for 1 h. The remaining GR activity was determined by GR assay after the incubation.

2.5 Kinetics of GR inhibition induced by NQ-6

The concentration- and time-dependence of GR inhibition by NQ-6 was evaluated to determine the parameters of enzyme inhibition kinetics. 0.6 U/mL GR in PE buffer containing 1 mg/mL BSA and 0.2 mM NADPH were incubated with various concentrations of NQ-6 (0, 4, 8, 16 µM) at 37°C. Aliquots were withdrawn and the remaining GR activity was analyzed at 10, 20, 30 and 40 min. The sample prepared without NQ-6 treatment was conducted in parallel as a control at 0 min. A total of 100 µL mixture containing 0.3 mM NADPH and 0.75 mM GSSG was added to 50 µL GR aliquot withdrawn above in a 96-well plate, and the remaining enzyme activity was determined. K_i and k_{inact} values were calculated based on the following formula of Kitz and Wilson [21, 22].

$$\frac{1}{K_{app}} = \left(\frac{1}{K_{inact}} + \frac{K_i}{K_{inact}}\right) \times \frac{1}{[I]}$$

2.6. Determination of the irreversibility of GR inhibition by dialysis of NQ-6-treated GR

6 U/mL GR was incubated with 100 µM NQ-6 in the presence of 0.2 mM NADPH at 37°C for 1 h, and then loaded into a Slide-A-Lyzer dialysis cassette (Thermo Scientific) with a molecular mass cut-off of 10 kDa followed by extensive dialysis in 500 mL PE buffer with continuous stirring. Control sample was prepared in the absence of NQ-6 treatment. Aliquots were withdrawn at different time intervals, and the remaining GR activity was determined as described for the GR activity assay.

2.7. Substrate protection assay

1.5 U/mL GR was incubated with 0.2 mM NADPH at 37°C for 1 h, and then the NADPH-pretreated GR was incubated with 20 µM NQ-6 in the presence or absence of GSSG (20, 40, 80 and 160 µM) in PE buffer at 37°C for 20 min. After incubation, aliquots without NADPH removal were withdrawn and the remaining GR activity was determined as described for the GR activity assay.

2.8. Determination of NQ-6-induced intracellular GR inhibition in human cancer cells

A375 and NUGC3 cells were treated with different concentrations of NQ-6 (10, 20, 40, and 60 µM) for 2 h. Control samples were processed in parallel without NQ-6 treatment. The cells were collected by trypsinization and washed twice with cold PBS and lysed in RIPA buffer on ice for 30 min. The lysate was centrifuged at 150,000 ×g for 30 min at 4°C. The supernatant was collected and used to determine GR activity as described above. The protein concentrations of the cell lysate were determined by the BCA assays and the GR activity was normalized to protein concentrations accordingly.

2.9. Reactive oxygen species (ROS) detection

Intracellular ROS generation was determined by using a CellRox Green Reagent fluorescent probe according to the manufacturer's instructions. The cells were treated with the indicated concentration of NQ-6 at 37°C for 2 h and then stained with 2.5 µM CellRox Green Reagent for 30 min. The intracellular green fluorescence intensity was analyzed by flow cytometry (SP6800, SONY). Data analysis was performed using FlowJo software.

2.10. In vivo study

ICR mice (5 weeks, male) were obtained from Shanghai SLAC Laboratory Animal Co. Ltd. (Shanghai, China). The animal

experiments followed the protocols approved by the Institutional Animal Care and Use Committee at Zhejiang Cancer Hospital. All the mice were housed in the animal facility of Zhejiang Cancer Hospital under a climate-controlled environment with a 12 h light/dark cycle. The mice were fasted for 12 h before experiment. NQ-6 and the positive control carmustine (BCNU) were prepared in 0.5% carboxymethylcellulose sodium solution and administrated to mice by oral gavage. Thirty minutes after administration, the mice were anesthetized by inhalation of isoflurane using an anesthesia machine and euthanized by cervical dislocation. The livers, spleens, lungs and kidneys of mice were collected and homogenized with a homogenizer. The homogenate was centrifuged at 150,000 ×g for 30 min at 4°C. The control samples were prepared from the naïve mice which were not administrated with vehicle nor compounds. The supernatant was collected and used to determine GR activity as described above.

2.11 GSH and GSSG quantification in cancer cells

Intracellular GSH and GSSG concentrations in cancer cells were determined by the established LC-MS method described earlier [17]. Briefly, the cancer cells treated with NQ-6 for 3 h were collected by trypsinization followed by cold PBS wash (1 mL × 2). And, then the intracellular GSH and GSSG were extracted by adding 0.1 mL of 3% (w/v) sulfosalicylic acid aqueous solution. The cell suspension was sonicated over ice for 5 min and centrifuged at 16,000 ×g for 10 min at 4°C and the supernatant was collected and diluted with 0.2% (w/v) formic acid and then submitted for GSH and GSSG analysis by LC-MS. GSH, GSSG and *p*-aminobenzoic acid (internal standard) at the mass of m/z 307.08381 $(M+H)^+$ m/z, 612.15196 $(M+H)^+$ m/z and 138.05550 $(M+H)^+$ m/z were detected by LC-MS in positive ionization and SIM (selected-ion monitoring) mode, respectively. The mass tolerance was set at 10 ppm.

2.12 Protein S-glutathionylation detection by immunofluorescence

The protein *S*-glutathionylation induced by NQ-6 in A375 and NUGC3 cells was detected using anti-glutathione antibody followed by probing by a green fluorescent-conjugated secondary antibody. Briefly, the cells were seeded at densities of 50,000 cells in an 8-well chamber slide. After 24-h attachment at 37°C, the cells were treated with various concentrations of NQ-6 for 1 h. The cells were washed with PBS twice and then fixed with 3.7% formaldehyde and prepared in PBS for 10 min at room temperature. The cells were washed 3 times with PBS and incubated with cell permeable solution (0.1% Na-citrate, 0.1% Triton-X-100 in PBS) at room temperature for 1 h. After incubation with the blocking solution (5% bovine serum albumin), the cells were incubated with anti-glutathione monoclonal antibody followed by probing by FITC-conjugated secondary antibody. The nuclei were stained with DAPI (1 μg/mL). Fluorescent images were taken with an Olympus IX53 fluorescent microscope.

2.13 LC-MS/MS analysis of NQ-6-treated GR

Yeast GR samples for mass spectrometric analysis were prepared as described earlier [23] with minor modifications. In brief, 8.0 μg yeast GR was incubated with the absence and presence of 100 μM NQ-6 in PE buffer containing NADPH at 37°C for 1 h. After incubation, the remaining NQ-6 was removed by an Amicon® Ultra 10 kDa molecular weight cut-off filter (Millipore, USA) by centrifugation. The GR samples were concentrated and denatured in 6 M urea at room temperature for 30 min. And then, the samples were digested with trypsin (1:50, w/w) in 25 mM ammonium bicarbonate solution at 37°C for overnight. The digested peptides were extracted and desalted by using Pierce® C18 Tips (Thermo Scientific, Rockford, IL, USA) following the manufactory protocol. The digested peptides were eluted from the C18 Tips by using 80% (v/v) acetonitrile aqueous solution and the solvent was removed under vacuum. The samples were reconstituted in 0.1% (v/v) TFA aqueous solution. The above 2 μg digested peptides were analyzed by a Q-Exactive Orbitrap high resolution mass spectrometer equipped with an Easy-nLC™ 1000 ultra-high pressure nano-HPLC system. The samples were separated on a C_{18} Acclaim® PepMap RSLC column (50 μm × 15 cm, 2 μm, 100 Å) (Thermofisher Scientific) coupled with a C_{18} Acclaim® PepMap 100 pre-column (100 μm × 2 cm, 5 μm, 100 Å) (Thermofisher Scientific), and then the eluted peptides were introduced into the mass spectrometer operating in tandem mass mode across a 90 min gradient [8% (v/v) acetonitrile/0.1% (v/v) formic acid to 25% acetonitrile/0.1% (v/v) formic acid in 70 min, 25% (v/v) acetonitrile/0.1% (v/v) formic acid to 45% (v/v) acetonitrile/0.1% (v/v) formic acid in 10 min, 45% (v/v) acetonitrile/0.1% (v/v) formic acid to 95% (v/v) acetonitrile/0.1% (v/v) formic acid in 3 min, and held at 95% (v/v) acetonitrile/0.1% (v/v) formic acid for another 7 min].

2.14 Detection of mitochondrial membrane potential (Δψm)

Δψm was detected with the tetramethylrhodamine ethyl ester (TMRE) staining kit (C2001S, Beyotime Biotech, China). The A375 and NUGC3 cells were treated with various concentrations of NQ-6 and CCCP as the positive control at 30 μM for 4 h. And, then the cells were loaded with the potentiometric dye TMRE at 37°C for 20 min [24] and fluorescent images were taken by an Olympus IX53 fluorescent microscope. The fluorescent intensity of TMRE was analyzed and quantified by ImageJ software. The cells processed in the same way were also analyzed by flow cytometry (SP6800, SONY). Data analysis was performed using FlowJo software.

2.15 Statistical analysis

Data were analyzed with GraphPad Prism software. The Student's *t*-test was performed to illustrate the differences between treatment groups and untreated controls. Each experiment was implemented at least triplicate. $P < 0.05$ was considered as significance in all experiments. Data were derived from at least three independent experiments and the values were expressed as mean ± SD or mean ± SEM.

3. Results

3.1 Inhibition of yeast GR by NQs

Purified yeast GR in PE buffer containing 1 mg/mL BSA and 0.2 mM NADPH was incubated with various concentrations

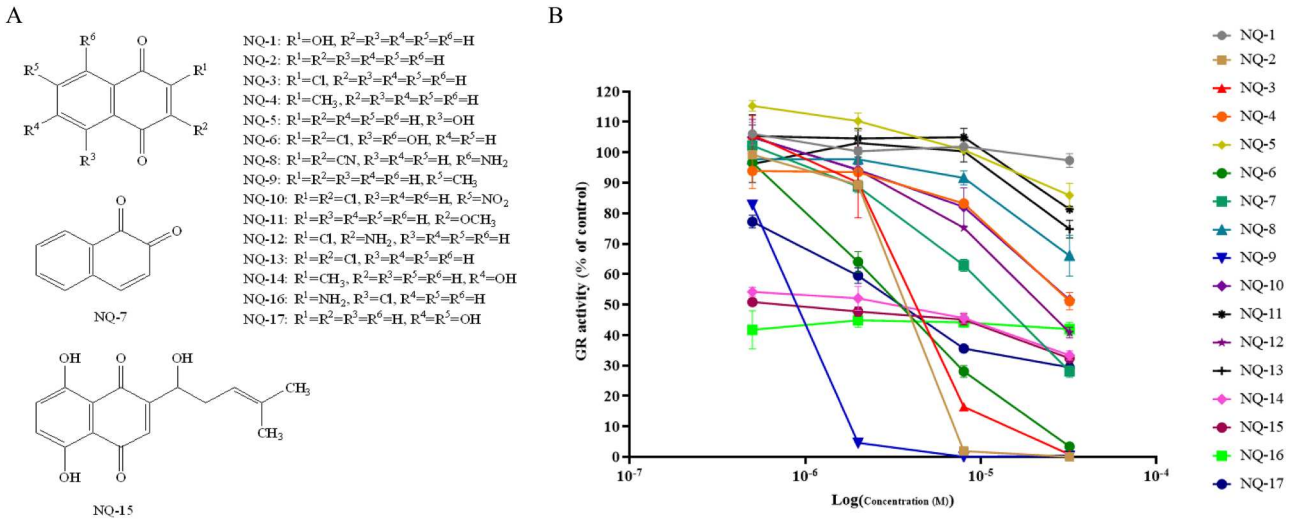

Figure 1. The chemical structures of the tested NQs (A) and their GR inhibitory effects (B). The results are presented as the means ± S.D. of three independent experiments.

of all the obtained 17 NQs compounds or without compounds (Figure 1A) at 37°C for 1 h. The remaining GR activity was determined by the GR assay. The results (Figure 1B) showed that the NQs inhibited yeast GR in a concentration-dependent manner. Take consideration of NQs' GR inhibitory potency against purified and intracellular GR, as well as the GR in organs of mice., The most potent top 4 NQs in Figure 1B were selected and tested *in vitro* and *in vivo* for GR inhibitory effects. As shown in Figure S1A, the top 3 NQs (NQ-2, NQ-3 and NQ-9) from Figure 1B showed much less inhibitory ability against intracellular GR of cancer cells compare to that of NQ-6 (Figure 4A). In addition, no GR inhibitory effect was observed in NQ-9-treated mice organs (Figure S1B). Preliminary experiments with NQ-6 revealed that it exhibited the most effective inhibitory impact on GR activity. NQ-6 was selected as the candidate compound to illustrate the inhibitory kinetics and the mechanism of action.

3.2 Kinetics of GR inhibition by NQ-6

The results indicated that GR was inhibited by NQ-6 in a concentration- and time-dependent manner as shown in Figure 2A, which presents a plot derived from the natural logarithm of the GR activity versus time at various concentrations of NQ-6. The results showed that NQ-6 induced GR activity repression over time, indicating a characteristic of irreversible enzyme inhibition. The inhibitory parameters K_i and k_{inact} of NQ-6 against yeast GR were determined to be 17.30 ± 3.63 μM and 0.0136 ± 0.0005 min^{-1} respectively by plotting the reciprocal of apparent rate constant of inhibition (k_{app}) (slopes calculated from Figure 2A) against the reciprocal of inhibitor concentration (Figure 2B) according to the method of Kitz and Wilson [21].

3.3 Irreversible GR inhibition induced by NQ-6

Dialysis of NQ-6-inhibited GR was performed to determine the irreversibility of the GR inhibition by NQ-6. The NQ-6-treated GR was extensively dialyzed in a bulky PE buffer. No GR activity rescue was observed in NQ-6-inhibited GR after 24 h-dialysis, confirming the possibility of irreversible inhibition of GR by NQ-6 (Figure 2C).

3.4 Substrate protection assay

The substrate protection assay was carried out in the absence and presence of substrate GSSG to investigate whether NQ-6 is a competitive inhibitor of GR and whether the inhibitor interferes with the catalytic center of GR. The results (Figure 2D) showed that GSSG significantly protected GR from inhibition by NQ-6 in a concentration-dependent manner revealing that NQ-6 and GSSG were competing for the same substrate binding site of GR and NQ-6 is a competitive inhibitor of GR.

3.5 Mass spectrometric analysis of NQ-6-GR complex

Yeast GR was incubated with the absence and presence of 100 μM NQ-6 in PE buffer containing NADPH at 37°C for 1 h followed by protein denature and trypsin digestion. The desalted samples were subjected to a Q-Exactive Orbitrap high resolution mass spectrometer equipped with an Easy-nLC™ 1000 ultra-high pressure nano-HPLC system. The LC-MS/MS raw data were analyzed by Proteome Discoverer 1.4 software (ThermoFisher). In the NQ-6-treated GR samples, the precursors of NQ-6-modified peptides TLLVEAKALGGTCVNVGCVPK and TLLVEAKALGGTCVNVGCVPKK containing the substrate binding sites Cys^{61} and Cys^{66} were detected (Figure 3A-D). The precursor ion at m/z 629.77655 $(M + 4H)^{4+}$ containing bis-NQ-6 adduct (2 × 221.97199 Da) was extracted from the mass spectrum (Figure 3C) at retention time of 46.75 min indicating that two substrate binding sites Cys^{61} and Cys^{66} of GR were modified by NQ-6 through covalent bind simultaneously. The precursor ion at m/z 606.29926 $(M + 4H)^{4+}$ containing mono-NQ-6 adduct (221.97199 Da) was extracted from the mass spectrum (Figure 3D) at retention time of 34.96 min indicating that one of the substrate binding sites Cys^{61} and Cys^{66} of GR was modified by NQ-6. By investigating the tandem mass of the monomer precursor ion at m/z 606.29926 $(M + 4H)^4$, a series of fragment ions were observed (Tables 1 & 2). A y6 ion (GCVPKK) was detected at m/z 285.11938 $(M + 3H)^3$ with mono-NQ-6 adduct (221.97199 Da) revealing that only the thiol on Cys^{66} was covalently modified by NQ-6 (Figure 3E). And, no NQ-6 modification was detected in the untreated GR samples (data not shown).

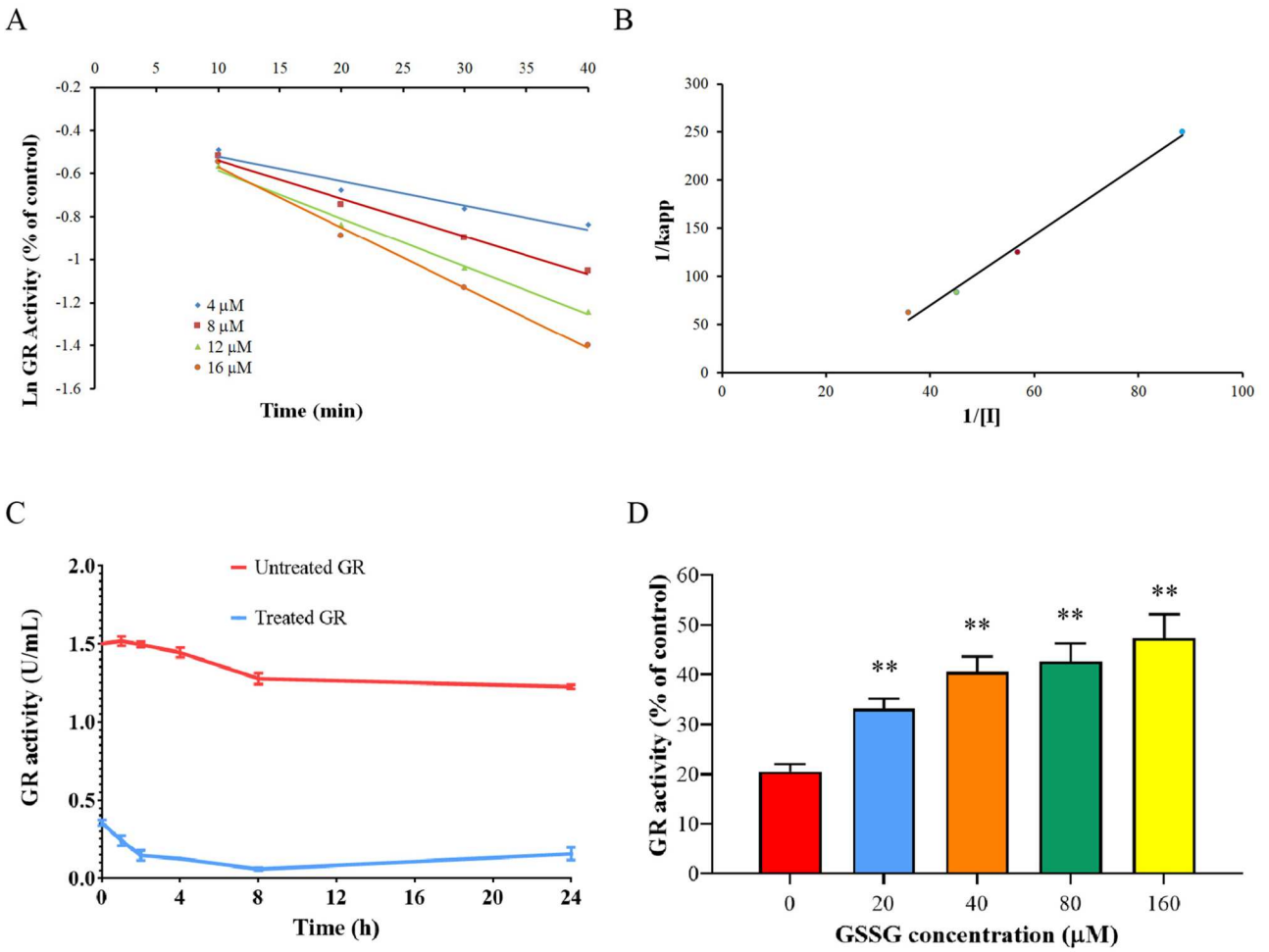

Figure 2. The inhibitory kinetics of GR by NQ-6. (A) time- and concentration-dependent inhibition of GR. The natural logarithm of remaining yGR activity (% of control) is plotted against time. The data were derived from one of the triplicate experiments. (B) Determination of K_i and k_{inact} based on the method of Kitz and Wilson [21]. Double-reciprocal plot of the apparent rate constants of inhibition (k_{app}, slope from A) versus the reciprocal of NQ-6 concentration ([*I*]). The K_i and k_{inact} values were calculated to be 17.30 ± 3.63 μM and 0.0136 ± 0.0005 min^{-1}, respectively. (C) Determination of the irreversibility of GR inhibition by NQ-6 via dialysis. NQ-6 treated yeast GR was extensively dialyzed in PE buffer in a Slide-A-Lyzer dialysis cassette with a molecular mass cut-off of 10 kDa. The data showed one of three independent experiments. (D) Substrate protection of GR against NQ-6 inhibition. NADPH-pretreated GR was incubated with 20 μM NQ-6 in the presence or absence of GSSG (0, 20, 40, 80 and 160 μM) in PE buffer at 37°C for 20 min. Aliquots were withdrawn and tested for GR activity as described for the GR assay. The results are presented as the means ± S.D. of three independent experiments. $^{**}P < 0.01$ versus control group.

3.6 Determination of intracellular GR inhibition in NUGC3 and A375 cells

To evaluate the inhibitory effect of NQ-6 on intracellular GR, NUGC3 and A375 cells were incubated with NQ-6 at 0, 10, 20, 40 and 60 μM concentrations. After treated for 2 h, the intracellular GR activity was significantly inhibited by NQ-6, indicating that NQ-6 was able to significantly suppress intracellular GR activity in these two cancer cell lines (Figure 4A).

3.7 Determination of GR inhibition in organs of ICR mice

NQ-6 and BCNU as the positive control prepared in 0.5% carboxymethylcellulose sodium solution were administrated to mice by oral gavage. Mice in the untreated group served as the controls. The GR activity in mouse liver, lung, spleen and kidney was analyzed. The results showed that NQ-6 at 10 mg/kg significantly reduced the GR activity in mice liver (Figure 4B) and spleen (Figure 4C), and NQ-6 at 20 mg/kg significantly reduced the GR activity in mice liver (Figure 4B), lung (Figure 4D) and kidney (Figure 4E). BCNU at 40 mg/kg only significantly suppressed GR activity in mice liver (Figure 4B) and kidney (Figure 4E), exhibiting poorer GR inhibitory effects than NQ-6.

3.8 NQ-6 induces thiol oxidative stress in cancer cells

The intracellular GSH and GSSG in NUGC3 and A375 cells were quantified using LC-MS. As shown in Figure 5A&D, depletion of GSH was only observed in cells treated with NQ-6. However, substantial increase in GSSG concentration was observed in A375 and NUGC3 cells (Figure 5B&E). Up to 2.5 and 2.3 fold-change of GSSG was determined in A375 and NUGC3 cells, respectively. The intracellular GSH/GSSG ratios, a major index reflecting intracellular thiol oxidative stress, were calculated and presented in Figure 5C&F. The GSH/GSSG ratio was determined to be 234.9 : 1 and 54.2 : 1 in A375 and NUGC3 cells, respectively. After treated with NQ-6, the GSH/GSSG ratio was significantly decreased to the range of 113.9 : 1–89.1: 1 in A375 cells and 21.1 : 1–11.7 : 1 in NUGC3 cells. The data indicated that NQ-6 is able to generate thiol oxidative stress by inducing of GSSG accumulation.

3.9 NQ-6 induces ROS generation in cancer cells

The intracellular ROS generation induced by NQ-6 in the NUGC3 and A375 cells was determined by flow cytometry. The results showed that NQ-6 induced significant ROS produce in these two cell lines. Compared to the controls,

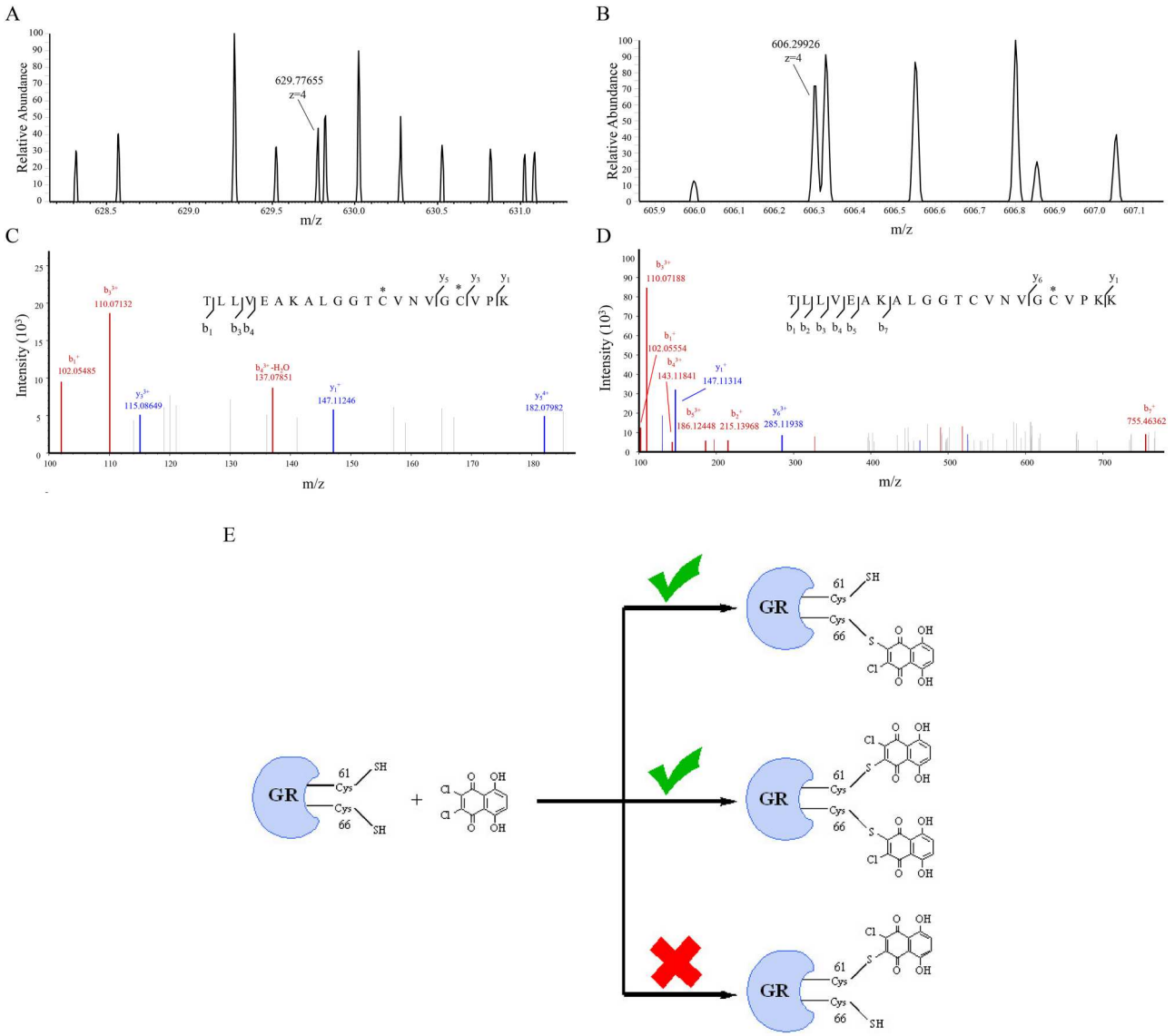

Figure 3. Mass spectra of NQ-6-treated yeast GR and the molecular mechanism of GR inhibition. NQ-6 treated yeast GR was denatured in 6 M urea and digested with trypsin (1:50, w/w) in 25 mM ammonium bicarbonate solution at 37°C for overnight. The digested peptides were extracted and desalted and submitted for LC-MS/MS analysis. The LC-MS/MS spectra were derived from the digested peptides of GR. (A) The precursor ion at m/z 629.77655 $(M + 4H)^{4+}$ containing bis-NQ-6 adduct (2×221.97199 Da) was extracted from the mass spectrum at retention time of 46.75 min. (B) The precursor ion at m/z 606.29926 $(M + 4H)^{4+}$ containing mono-NQ-6 adduct (221.97199 Da) was extracted from the mass spectrum at retention time of 34.96 min. (C,D) Fragmentation of precursor ion at m/z 629.77655 $(M + 4H)^{4+}$ and precursor ion at m/z 606.29926 $(M + 4H)^{4+}$ from trypsin-digested NQ-6-treated GR, respectively. (E) Proposed mechanism of yeast GR inhibition by NQ-6. The tandem mass analysis of the NQ-6-inhibited yeast GR revealed that the thiol on Cys^{61} and Cys^{66} can be covalently modified by NQ-6 simultaneously or only Cys^{66} is covalently modified by NQ-6.

the ROS level was increased up to 1.55 and 2.07-fold in the A375 (Figure 5G,H) and NUGC3 (Figure 5I,J) cells treated with 20 μM NQ-6, respectively.

3.10 NQ-6 induces protein S-glutathionylation in cancer cells

Protein *S*-glutathionylation was found to be induced in cancer cells earlier by GR inhibitor 2-AAPA [20, 25]. Protein *S*-glutathionylation detection was performed to reveal whether NQ-6 is able to increase the intracellular *S*-glutathionylation of cancer cells. The result showed that protein *S*-glutathionylation was elevated by NQ-6 treatment in A375 and NUGC3 cells (Figure 6).

Table 1. Observed fragment ions of peptide -TLLVEAKALGGTC*VNVGC*VPK in the tandem mass spectrum of trypsin-digested NQ-6-treated Yeast GR.

Observed ions	Theoretical (*m/z*)	Observed (*m/z*)
TLLVEAKALGGTC*VNVGC*VPK	629.77307 (M + 4H)	629.77655 (M + 4H)
T (b_1)	102.05496 (M + H)	102.05485 (M + H)
TLL (b_3)	110.07922 (M + 3H)	110.07132 (M + 3H)
TLLV-H_2O (b_4-H_2O)	137.09850 (M + 3H)	137.07851 (M + 3H)
K (y_1)	147.11281 (M + H)	147.11246 (M + H)
VPK (y_3)	115.08285 (M + 3H)	115.08649 (M + 3H)
GC*VPK (y_5)	182.06462 (M + 4H)	182.07982 (M + 4H)

*NQ adduct.

3.11 NQ-6 induces mitochondrial membrane potential (Δψm) depletion in cancer cells

TMRE staining was performed to determine the changes in Δψm by NQ-6 in cancer cells. TMRE only accumulates in hyperpolarized mitochondria, and its red fluorescent intensity correlates with mitochondrial membrane potential. As shown in Figure 7, NQ-6 treatment induced a concentration-dependent depletion of Δψm in both A375 and NUGC3 cells. NQ-6 increased a significant decline in red fluorescent intensity in these two cell lines (Figure 7A, B), which indicated the Δψm loss. The mitochondrial membrane potential collapse was found to be from 10.0% to 95.4% and 9.8% to 96.2% in

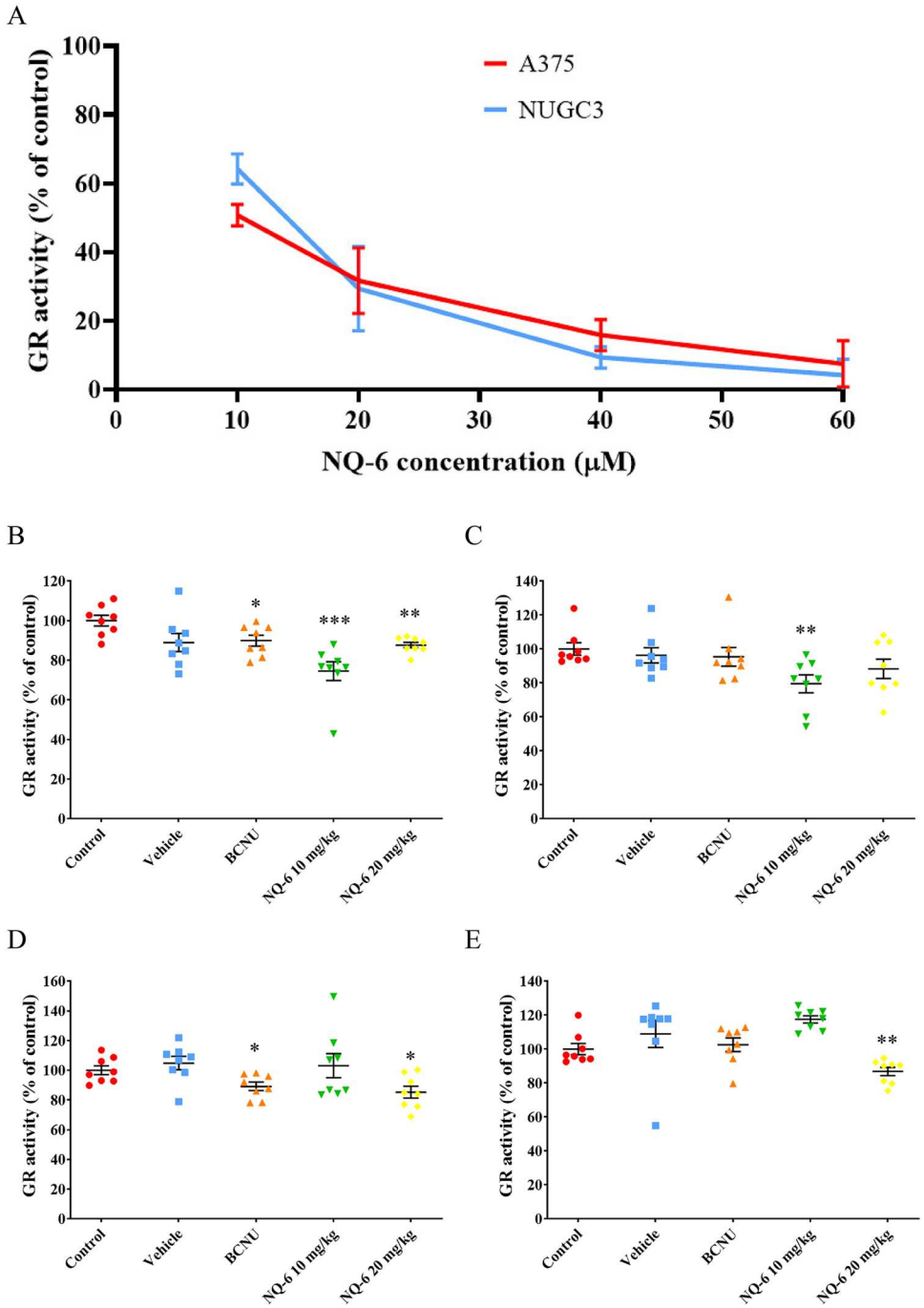

Figure 4. Inhibition of GR *in vitro* and *in vivo* by NQ-6. NQ-6-induced GR inhibition was tested *in vitro* and *in vivo*. (A) The intracellular GR is inhibited by NQ-6 in A375 and NUGC3 cells. The cells were treated with different concentrations of NQ-6 (10, 20, 40, and 60 μM) for 2 h and collected by trypsinization and lysed in RIPA buffer. The supernatant was obtained by centrifugation and tested for GR activity. The results are shown as the means ± S.D. of three independent experiments. NQ-6 and the positive control carmustine (BCNU) were prepared in 0.5% carboxymethylcellulose sodium solution and administrated to mice by oral gavage. The mice were anesthetized by inhalation of isoflurane and euthanized by cervical dislocation. The organs of mice were collected and homogenized. The supernatant was collected and tested for GR activity as described above. NQ-6 reduced the GR activity in mice (B) liver, (C) spleen, (D) lung and (E) kidney.

A375 and NUGC3 cells treated with NQ-6, respectively. The positive control CCCP caused 39.1% and 23.3% mitochondrial membrane potential lose in A375 and NUGC3 cells, respectively. Depletion of Δψm in these two cell lines treated with NQ-6 was confirmed by flow cytometric analysis (Figure 7C, D). Significant changes of TMRE-negative cell amount were observed in NQ-6 treated A375 and NUGC3 cells. The results indicated that NQ-6 was more potent in depletion of Δψm in cancer cells than CCCP with comparable concentrations. In the meantime, the cells submitted for flow cytometric assay were stained with trypan blue and the cell viability was determined by a cell counter (Countess 3 FL, Invitrogen, Thermo Fisher Scientific). The results shown in Figure

Table 2. Observed fragment ions of peptide -TLLVEAKALGGTCVNVGC*VPKK in the tandem mass spectrum of trypsin-digested NQ-6-treated Yeast GR.

Observed ions	Theoretical (*m/z*)	Observed (*m/z*)
TLLVEAKALGGTCVNVGC*VPKK	606.30381 (M + 4H)	606.29926 (M + 4H)
T (b_1)	102.05496 (M + H)	102.05554 (M + H)
TL(b_2)	215.13903 (M + H)	215.13968 (M + H)
TLL (b_3)	110.07922 (M + 3H)	110.07188 (M + 3H)
TLLV (b_4)	143.10202 (M + 3H)	143.11841 (M + 3H)
TLLVE (b_5)	186.11622 (M + 3H)	186.12448 (M + 3H)
TLLVEAK (b_7)	755.46621 (M + H)	755.46362 (M + H)
K (y_1)	147.11281 (M + H)	147.11314 (M + H)
VGC*VPK (y_6)	285.11539 (M + 3H)	285.11938 (M + 3H)

*NQ adduct.

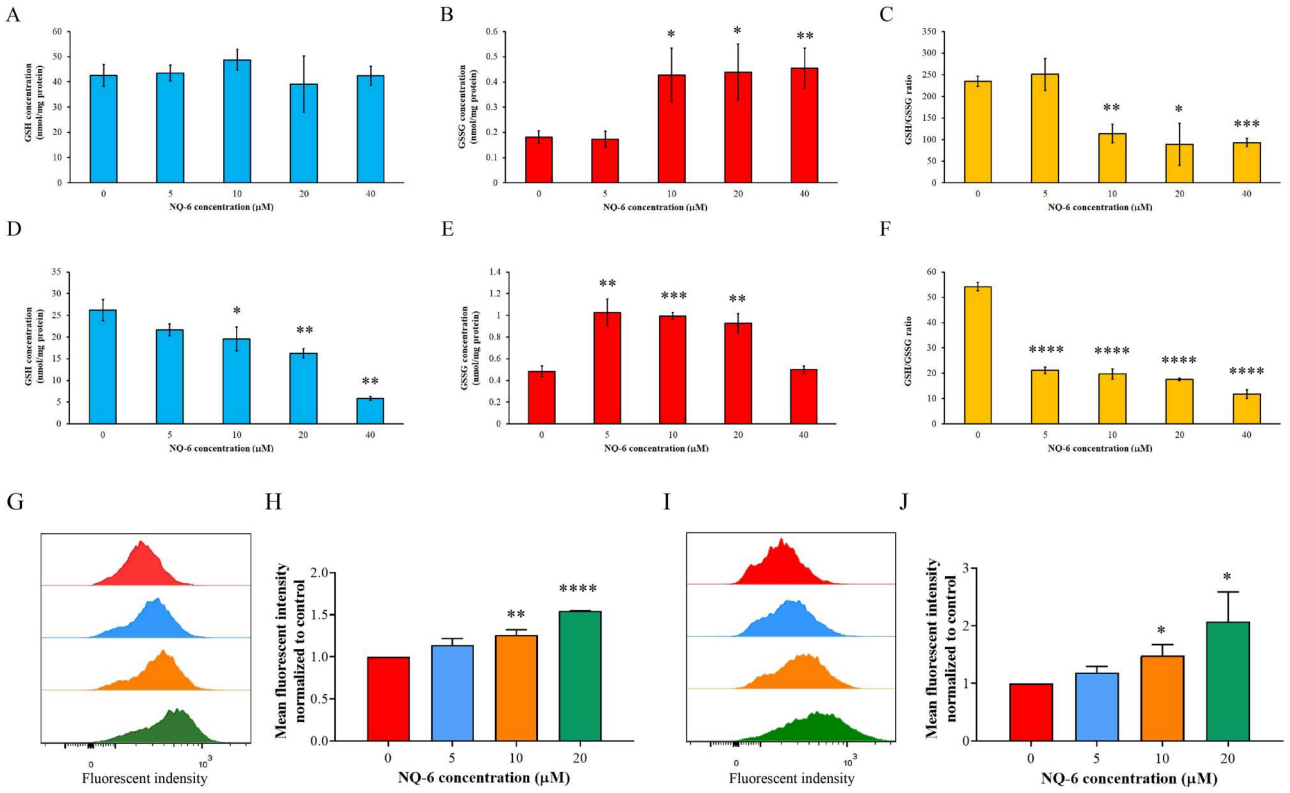

Figure 5. NQ-6 induced oxidative stress in cancer cells. NQ-6 induced thiol oxidative stress in A375 (A-C) and NUGC3 (D-F) cells. The cancer cells were treated with various concentrations of NQ-6 at 37°C for 3 h. Intracellular GSH, GSSG, and GSH/GSSG ratios were detected by LC-MS. NQ-6 stimulated ROS generation in A375 (G-H) and NUGC3 (I,J) cells. The NQ-6-treated cells were stained with 2.5 μM CellRox Green Reagent. The intracellular green fluorescence intensity was analyzed by flow cytometry. Data analysis was performed using FlowJo software. The results are presented as the means ± S.D. of three independent experiments. *$P < 0.05$; **$P < 0.01$; ***$P < 0.001$; ****$P < 0.0001$versus control group.

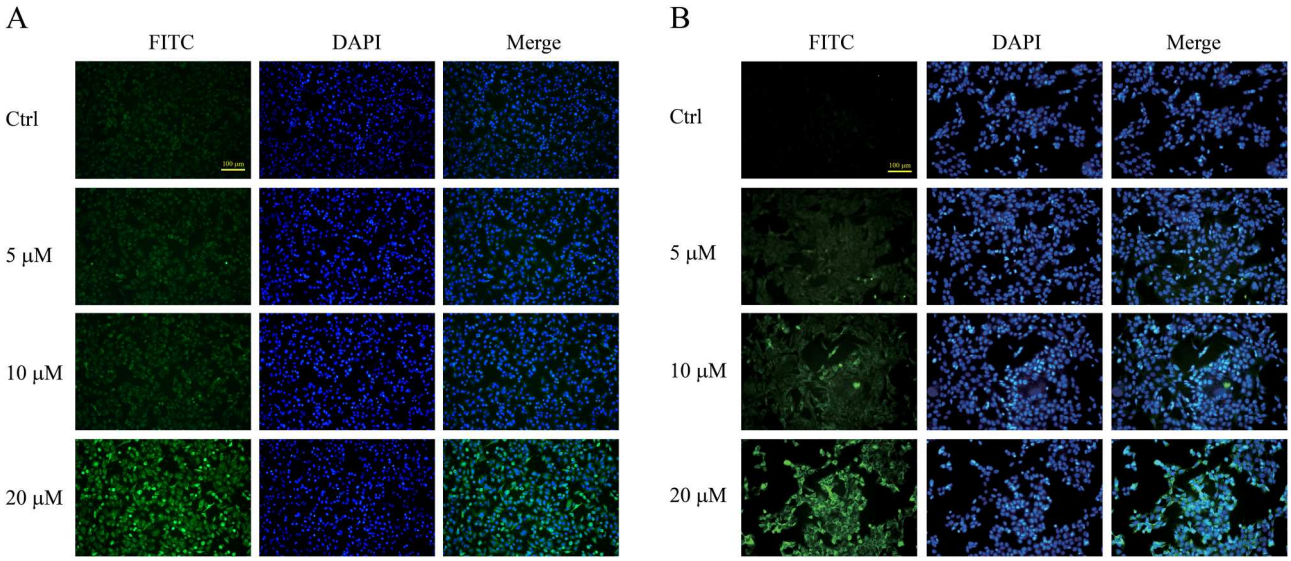

Figure 6. Protein *S*-glutathionyaltion induced by GR inhibition in the A375 (A) and NUGC3 (B) cells. The cancer cells were treated with NQ-6 at the indicated concentrations for 1 h and the *S*-glutathionylation was recognized by anti-glutathione antibody and probed by FITC-conjugated second antibody and nuclei were stained with DAPI. Fluorescent images were captured by an Olympus IX53 fluorescent microscope. The data are derived from one of the three independent experiments.

S2 ensured that the majority of the cells submitted for flow cytometric analysis were live cells.

4. Discussions

Naphthoquinones are naturally distributed secondary metabolites and highly reactive small molecules [26]. In the present study, we have shown that a series of NQs are capable of inhibiting yeast GR, intracellular GR in human cancer cells and GR in the organs of ICR mice.

During screening this series NQs' GR inhibitory capability, several NQ compounds (such as NQ-2, NQ-3 and NQ-9) were found to be more potent than NQ-6. Somehow, they were unable to inhibit intracellular GR efficiently (data not shown). Therefore, NQ-6 was selected as the representative NQ among this series to illustrate the inhibitory kinetics and

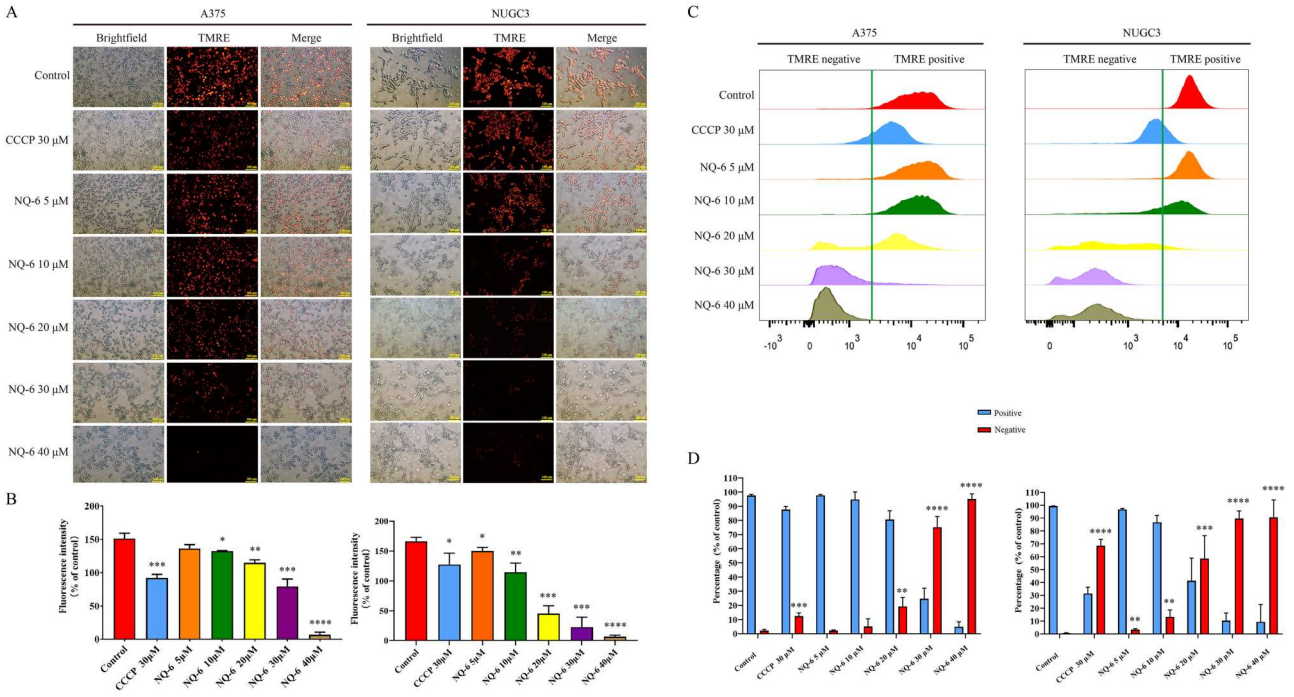

Figure 7. NQ-6 induced mitochondrial membrane potential (*Δψm*) changes in the cancer cells. The A375 and NUGC3 cells were treated with various concentrations of NQ-6 and CCCP as the positive control at 30 μM for 4 h. Δψm was probed by TMRE followed by analyzing using fluorescent microscopy (A,B) and flow cytometry (C, D). *$P < 0.05$; **$P < 0.01$; ***$P < 0.001$; ****$P < 0.0001$versus control group.

the mechanism of action. NQ-6 exhibited a time- and concentration-dependent inhibitory manner against yeast GR. The inhibitory parameters K_i and k_{inact} of NQ-6 against yeast GR were calculated to be 17.30 ± 3.63 μM and 0.0136 ± 0.0005 min^{-1}, respectively. Based on the results, NQ-6 is more potent and effective than BCNU and 2-AAPA, two widely used GR inhibitors, in inhibiting GR [22, 27]. The dialysis experiment further indicated that GR inhibition induced by NQ-6 was probably irreversible. The GR inhibition by NQ-6 was prevented by addition of substrate GSSG, indicating that the inhibitor was competing with the substrate and interacting with the active site of GR. All the above results indicated that covalent modifications between NQ-6 and the thiol groups of cysteine residues at the active site of the GR enzyme may have been formed. To identify which active site residues Cys^{61} and/or Cys^{66} are covalently modified by NQ-6, the samples were processed and submitted for LC-MS/MS analysis. The tandem mass spectrometric analysis revealed that the two substrate binding sites Cys^{61} and Cys^{66} of yeast GR were simultaneously modified through covalent bind or only Cys^{66} was covalently modified by NQ-6. Based on the tandem mass spectrometric data, we speculate that the thiol group in Cys^{66} in yeast GR is more active than Cys^{61} to be arylated by NQ-6. But whether the arylation on Cys^{66} can further facilitate covalent bond formation by NQ-6 on Cys^{61} is unknown. The irreversible inhibition of GR by NQ-6 was further confirmed by the LC-MS/MS results.

GR has become an attractive target for anticancer development. GR inhibitors have shown to possess anticancer potency, for example, FDA-approved BCNU exerted strong GR inhibitory activity and therapeutic cytotoxic effects [16]. GR inhibition was also found to be relevant to intracellular oxidative stress induction, suppression of cancer cell metastasis and chemo-resistance reversal [17, 20]. In this study, the capability of NQ-6 in inducing oxidative stress *in vitro* and *in vivo* was assessed. First of all, NQ-6's GR inhibitory effect was tested *in vitro* and *in vivo*. The results showed that NQ-6 significantly repressed GR activity in A375 and NUGC3 cells. GR inhibition was also observed in the liver, lung, spleen and kidney of ICR mice administrated with NQ-6. NQ-6 depleted GSH in NUGC3 cells rather than A375 cells. And GSSG concentration in A375 and NUGC3 cells increased significantly. As a result, the ratio of GSH/GSSG, a crucial marker of thiol oxidative stress, decreased dramatically indicating the generation of thiol oxidative stress by NQ-6 in these two cell lines. Moreover, the flow cytometric data showed that the ROS production probed by CellRox Green Reagent was also increased in A375 and NUGC3 cells treated with NQ-6. Mitochondria are known as the major intracellular source of ROS. In consequence, collapsing of mitochondrial membrane potential (Δψm) was observed in cancer cells treated with NQ-6. NQ-6 is more potent in inducing Δψm loss compared to CCCP at comparable concentrations. Protein *S*-glutathionylation, a unique redox-driven protein post-translational modification involving the reversible addition of a GSH to the cysteine residue through a disulfide bond, was found to be raised under thiol oxidative stress in various cancers [17, 28–31]. *S*-glutathionylation not only protects the reduced protein thiols from irreversible oxidation but also modulates various molecular and cellular signalling pathways by changing the structure and/or function of target proteins under physiological and pathological conditions [30, 32]. Protein *S*-glutathionylation is reported as a molecular mechanism associated with protein degradation in response to ROS and serves as cancer biomarkers [18, 31, 33]. As a result of GR inhibition, protein *S*-glutathionylation was observed increased significantly in the cancer cells treated with NQ-6. The results indicated the ability of NQs in induction of intracellular protein *S*-glutathionylation and may serve as a potential inducer of protein *S*-glutathionylation. All the data showed that NQs can be a useful research

tool to study the impact of GR inhibition on thiol status, protein *S*-glutathionylation and oxidative-related disease *in vitro* and *in vivo* [34, 35].

NQ derivatives were utilized in the treatment of various diseases, and mixtures were well-tolerated by the patients and no signs of heart, kidney, and liver toxicities were reported [36–38]. Early research revealed that the severity of side effects induced by NQ derivatives is significantly lower than those caused by the parent compound at the same dosage level [39]. Therefore, most of the NQs demonstrated low toxicity potential. Some animal experiments showed that the most effective dosage of NQ compounds is significantly lower than the toxic dose [40]. With no alterations in body weight or animal behavior observed, continuous administration of high doses, reaching up to 10 mg/kg/day for 21 days, did not induce significant side effects. Consequently, NQ compounds could potentially exhibit a favorable therapeutic index in clinical treatments [40, 41].

5. Conclusions

In summary, NQs have been characterized as irreversible and competitive inhibitors of GR. NQ-6 inhibited yeast GR activity by arylating the thiol/thiols on Cys^{66} along or two substrate binding sites Cys^{61} and Cys^{66} simultaneously. In addition, NQ-6 can repress GR activity in the cancer cells and the organs of ICR mice. The data revealed that NQ-6 induced thiol oxidative stress, ROS, collapsing of mitochondrial membrane potential and protein *S*-glutathionylation in the cancer cells by inhibition GR.

Disclosure statement

No potential conflict of interest was reported by the authors.

Funding

This work was supported by National Natural Science Foundation of China (82474120), Zhejiang Province Traditional Chinese Medicine Technology Project (2025051550), Zhejiang Provincial Natural Science Foundation (ZCLQ24B0502), Key Laboratory of Prevention, Diagnosis and Therapy of Upper Gastrointestinal Cancer of Zhejiang Province.

Data availability statement

The data that support the findings of this study are available from the corresponding author (Wei Chen), upon reasonable request.

ORCID

Wei Chen http://orcid.org/0000-0003-0801-5613

References

[1] Duran AG, Chinchilla N, Simonet AM, et al. Biological activity of naphthoquinones derivatives in the search of anticancer lead compounds. Toxins (Basel). 2023;15(5):348. doi:10.3390/toxins15050348
[2] Lozynskyi A, Senkiv J, Ivasechko I, et al. 1,4-Naphthoquinone motif in the synthesis of new thiopyrano[2,3-d]thiazoles as potential biologically active compounds. Molecules. 2022;27(21):7575. doi:10.3390/molecules27217575
[3] Futuro DO, Ferreira PG, Nicoletti CD, et al. The antifungal activity of naphthoquinones: an integrative review. An Acad Bras Cienc. 2018;90(1 Suppl 2):1187–1214. doi:10.1590/0001-3765201820170815
[4] Nunes JA, da Silva Nunes AF, da Paz Lima DJ, et al. Naphthoquinone derivatives targeting melanoma. Curr Top Med Chem. 2023;23(30):2863–2876. doi:10.2174/1568026623666230901124059
[5] Rahman MM, Islam MR, Akash S, et al. Naphthoquinones and derivatives as potential anticancer agents: an updated review. Chem Biol Interact. 2022;368:110198. doi:10.1016/j.cbi.2022.110198
[6] Valko M, Rhodes CJ, Moncol J, et al. Free radicals, metals and antioxidants in oxidative stress-induced cancer. Chem Biol Interact. 2006;160(1):1–40. doi:10.1016/j.cbi.2005.12.009
[7] Sies H, Jones DP. Reactive oxygen species (ROS) as pleiotropic physiological signalling agents. Nat Rev Mol Cell Biol. 2020;21(7):363–383. doi:10.1038/s41580-020-0230-3
[8] Cheung EC, Vousden KH. The role of ROS in tumour development and progression. Nat Rev Cancer. 2022;22(5):280–297. doi:10.1038/s41568-021-00435-0
[9] Perillo B, Di Donato M, Pezone A, et al. ROS in cancer therapy: the bright side of the moon. Exp Mol Med. 2020;52(2):192–203. doi:10.1038/s12276-020-0384-2
[10] Hayes JD, Dinkova-Kostova AT, Tew KD. Oxidative stress in cancer. Cancer Cell. 2020;38(2):167–197. doi:10.1016/j.ccell.2020.06.001
[11] Iqbal MJ, Kabeer A, Abbas Z, et al. Interplay of oxidative stress, cellular communication and signaling pathways in cancer. Cell Commun Signal. 2024;22(1):7. doi:10.1186/s12964-023-01398-5
[12] Guller P, Karaman M, Guller U, et al. A study on the effects of inhibition mechanism of curcumin, quercetin, and resveratrol on human glutathione reductase through *in vitro* and *in silico* approaches. J Biomol Struct Dyn. 2021;39(5):1744–1753. doi:10.1080/07391102.2020.1738962
[13] Ciftci E, Turkoglu V, Bas Z. Inhibition effect of thymoquinone and lycopene compounds on glutathione reductase enzyme activity purified from human erythrocytes. J Biomol Struct Dyn. 2022;40(20):10086–10093. doi:10.1080/07391102.2021.1939787
[14] Xiong Y, Xiao C, Li Z, et al. Engineering nanomedicine for glutathione depletion-augmented cancer therapy. Chem Soc Rev. 2021;50(10):6013–6041. doi:10.1039/D0CS00718H
[15] Niu B, Liao K, Zhou Y, et al. Application of glutathione depletion in cancer therapy: enhanced ROS-based therapy, ferroptosis, and chemotherapy. Biomaterials. 2021;277:121110. doi:10.1016/j.biomaterials.2021.121110
[16] Zhang R, Xiao N, Xu Q, et al. Pleiotropic effects of a mitochondrion-targeted glutathione reductase inhibitor on restraining tumor cells. Eur J Med Chem. 2023;248:115069. doi:10.1016/j.ejmech.2022.115069
[17] Li X, Wu J, Zhang X, et al. Glutathione reductase-mediated thiol oxidative stress suppresses metastasis of murine melanoma cells. Free Radic Biol Med. 2018;129:256–267. doi:10.1016/j.freeradbiomed.2018.07.025
[18] Li X, Ma Y, Wu J, et al. Thiol oxidative stress-dependent degradation of transglutaminase2 via protein S-glutathionylation sensitizes 5-fluorouracil therapy in 5-fluorouracil-resistant colorectal cancer cells. Drug Resist Updat. 2023;67:100930.
[19] Wellington KW. Understanding cancer and the anticancer activities of naphthoquinones – a review. RSC Adv. 2015;5(26):20309–20338. doi:10.1039/C4RA13547D
[20] Seefeldt T, Dwivedi C, Peitz G, et al. 2-Acetylamino-3-[4-(2-acetylamino-2-carboxyethylsulfanylcarbonylamino)- phenylcarbamoylsulfanyl]propionic acid and its derivatives as a novel class of glutathione reductase inhibitors. J Med Chem. 2005;48(16):5224–5231. doi:10.1021/jm050030i
[21] Kitz R, Wilson IB. Esters of methanesulfonic acid as irreversible inhibitors of acetylcholinesterase. J Biol Chem. 1962;237:3245–3249. doi:10.1016/S0021-9258(18)50153-8
[22] Seefeldt T, Zhao Y, Chen W, et al. Characterization of a novel dithiocarbamate glutathione reductase inhibitor and its use as a tool to modulate intracellular glutathione. J Biol Chem. 2009;284(5):2729–2737. doi:10.1074/jbc.M802683200
[23] Li X, Ni M, Xu X, et al. Characterisation of naturally occurring isothiocyanates as glutathione reductase inhibitors. J Enzyme Inhib Med Chem. 2020;35(1):1773–1780. doi:10.1080/14756366.2020.1822828
[24] Ni XC, Wang HF, Cai YY, et al. Ginsenoside Rb1 inhibits astrocyte activation and promotes transfer of astrocytic mitochondria to neurons against ischemic stroke. Redox Biol. 2022;54:102363. doi:10.1016/j.redox.2022.102363
[25] Chen W, Seefeldt T, Young A, et al. Microtubule *S*-glutathionylation as a potential approach for antimitotic agents. BMC Cancer. 2012;12:245. doi:10.1186/1471-2407-12-245

[26] Ahmadi ES, Tajbakhsh A, Iranshahy M, et al. Naphthoquinone derivatives isolated from plants: recent advances in biological activity. Mini-Rev Med Chem. 2020;20(19):2019–2035. doi:10.2174/1389557520666200818212020

[27] FitzGerald GB, Bauman C, Hussoin MS, et al. 2,4-Dihydroxybenzylamine: a specific inhibitor of glutathione reductase. Biochem Pharmacol. 1991;41(2):185–190. doi:10.1016/0006-2952(91)90475-K

[28] Mustafa Rizvi SH, Shao D, Tsukahara Y, et al. Oxidized GAPDH transfers *S*-glutathionylation to a nuclear protein sirtuin-1 leading to apoptosis. Free Radical Biol Med. 2021;174:73–83. doi:10.1016/j.freeradbiomed.2021.07.037

[29] Yang Y, Dong X, Zheng S, et al. GSTpi regulates VE-cadherin stabilization through promoting *S*-glutathionylation of Src. Redox Biol. 2020;30:101416. doi:10.1016/j.redox.2019.101416

[30] Hossain MS, Yao A, Qiao X, et al. Gbb glutathionylation promotes its proteasome-mediated degradation to inhibit synapse growth. J Cell Biol. 2023;222(9). doi:10.1083/jcb.202202068

[31] Pal D, Rai A, Checker R, et al. Role of protein *S*-glutathionylation in cancer progression and development of resistance to anti-cancer drugs. Arch Biochem Biophys. 2021;704:108890. doi:10.1016/j.abb.2021.108890

[32] Dalle-Donne I, Rossi R, Colombo G, et al. Protein *S*-glutathionylation: a regulatory device from bacteria to humans. Trends Biochem Sci. 2009;34(2):85–96. doi:10.1016/j.tibs.2008.11.002

[33] Munkanatta Godage DNP, VanHecke GC, Samarasinghe KTG, et al. SMYD2 glutathionylation contributes to degradation of sarcomeric proteins. Nat Commun. 2018;9(1):4341. doi:10.1038/s41467-018-06786-x

[34] Guo C, He J, Song X, et al. Pharmacological properties and derivatives of shikonin—a review in recent years. Pharmacol Res. 2019;149:104463.

[35] Fan S, Yan X, Hu X, et al. Shikonin blocks CAF-induced TNBC metastasis by suppressing mitochondrial biogenesis through GSK-3β/NEDD4-1 mediated phosphorylation-dependent degradation of PGC-1α. J Exp Clin Cancer Res. 2024;43(1):180.

[36] de Luna Martins D, Borges AA, Nada ES, et al. P2x7 receptor inhibition by 2-amino-3-aryl-1,4-naphthoquinones. Bioorg Chem. 2020;104:104278. doi:10.1016/j.bioorg.2020.104278

[37] Guo XP, Zhang XY, Zhang SD. Clinical trial on the effects of shikonin mixture on later stage lung cancer. Zhong Xi Yi Jie He Za Zhi. 1991;11(10):598–599. 580.

[38] Kim HK, Vasileva EA, Mishchenko NP, et al. Multifaceted clinical effects of echinochrome. Mar Drugs. 2021;19(8):412.

[39] Munday R, Smith BL, Munday CM. Toxicity of 2,3-dialkyl-1,4-naphthoquinones in rats: comparison with cytotoxicity *in vitro*. Free Radical Biol Med. 1995;19(6):759–765. doi:10.1016/0891-5849(95)00085-C

[40] Tripathi SK, Panda M, Biswal BK. Emerging role of plumbagin: cytotoxic potential and pharmaceutical relevance towards cancer therapy. Food Chem Toxicol. 2019;125:566–582. doi:10.1016/j.fct.2019.01.018

[41] Abedinpour P, Baron VT, Chrastina A, et al. Plumbagin improves the efficacy of androgen deprivation therapy in prostate cancer: a preclinical study. Prostate. 2017;77(16):1550–1562. doi:10.1002/pros.23428